Heliyon 10 (2024) e39554

Contents lists available at ScienceDirect

Heliyon

journal homepage: www.cell.com/heliyon

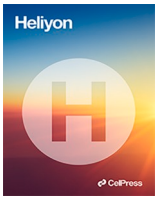

Research article

Untargeted metabolomics combined with pseudotargeted lipidomics revealed the metabolite profiles of blood-stasis syndrome in type 2 diabetes mellitus

Li Liu [a], Yuan-bin Liang [a], Xiao-lin Liu [a], Hong-qin Wang [b], Yi-fei Qi [b], Min Wang [c], Bao-xin Chen [d], Qing-bing Zhou [b,**], Wen-xin Tong [b,***], Ying Zhang [b,*]

[a] *Graduate School, China Academy of Chinese Medical Sciences, Beijing, 100700, China*
[b] *Institute of Geriatric Medicine, Xiyuan Hospital, China Academy of Chinese Medical Sciences, Beijing, 100091, China*
[c] *Beijing University of Chinese Medicine, Beijing, 100029, China*
[d] *Second Department of Encephalopathy, Dongfang Hospital, Beijing University of Chinese Medicine, Beijing, 100078, China*

A R T I C L E I N F O

Keywords:
Type 2 diabetes mellitus (T2DM)
Blood-stasis syndrome (BSS)
Untargeted metabolomics
Pseudotargeted lipidomics
Glycerophospholipids (GPs)
Fatty acyls (FAs)

A B S T R A C T

Objective: Blood-stasis syndrome (BSS), an important syndrome in Type 2 diabetes mellitus (T2DM), is associated with the pathophysiological mechanisms underlying diabetic vascular complications. However, BSS has not been fully characterized as of yet. Due to the strong correlation between BSS and vasculopathy, we hypothesized that the metabolic characteristics of BSS in T2DM (T2DM BSS) are highly specific. By combining untargeted metabolomics and pseudotargeted lipidomics approaches, this study aimed to comprehensively elucidate the metabolic traits of T2DM BSS, thereby providing novel insights into the vascular complications of diabetes and establishing a foundation for precision medicine.

Methods: The survey was conducted in Haidian District of Beijing from October 2021 to November 2021, and data collection was completed in January 2022. Liquid chromatography-mass spectrometry (LC-MS) based untargeted metabolomics and liquid chromatography-tandem mass spectrometry (LC-MS/MS) based pseudotargeted lipidomics were performed to detect metabolites and lipids. Multivariate, univariate, and pathway analyses were utilized to investigate metabolic changes. The unique metabolites of BSS were obtained by inter-group comparisons and screening. Receiver operating characteristic (ROC) curve analysis was performed to evaluate the diagnostic accuracy of metabolites.

Results: A total of 1189 participants completed the survey, of which 120 participants were recruited in this study and further divided into a discovery cohort (n = 90) and a validation cohort (n = 30). Among these, 21 participants were selected for psuedotargeted lipidomics analysis. 81 metabolites, mainly involving glycerophospholipids, were identified as unique metabolites of T2DM BSS, while fatty acyls (FAs) were identified as unique lipids. T2DM BSS was associated with significant dysregulation in glycerophospholipid metabolism and choline metabolism within cancer pathways as major metabolic disturbances. Furthermore, analyses of both the discovery and validation cohorts, indicated that LysoPC (20:5(5Z,8Z,11Z,14Z,17Z)/0:0) and LysoPC (15:0) had the greatest impact on distinguishing BSS.

* Corresponding author.
** Corresponding author.
*** Corresponding author.
E-mail addresses: zhouqingbing0910@163.com (Q.-b. Zhou), twx010@163.com (W.-x. Tong), zytgzhuanyong@163.com (Y. Zhang).

https://doi.org/10.1016/j.heliyon.2024.e39554
Received 1 February 2024; Received in revised form 17 October 2024; Accepted 17 October 2024
Available online 18 October 2024

Conclusion: Altered levels of glycerophospholipids and FAs have been associated with T2DM BSS. These results provide valuable mechanistic insights linked with the development of BSS in T2DM subjects.

1. Introduction

Type 2 diabetes mellitus (T2DM), a classical metabolic disease, is a multifaceted and chronic illness primarily driven by insulin resistance as the main underlying pathophysiological mechanism [1]. Of particular concern is the coexistence of T2DM with vascular complications [2], such as atherosclerotic cardiovascular disease (ASCVD), which significantly affects the patients' quality of life and mortality rates and shows an exceptionally high incidence. However, the mechanisms underlying these complications remain largely unexplored.

The theory of Yin-Yang and Five-Element is the philosophical foundation for Traditional Chinese Medicine (TCM) to understand the nature of diseases [3]. Different diseases, organs and individuals have different Yin, Yang and Five-Elements attributes. These attributes determine the clinical characteristics of patients. Based on the classification of the characteristics, syndrome differentiation is generated. TCM syndrome represents the generalization of disease conditions. Personalized therapeutic methods are selected on the basis of syndrome differentiation (Bian Zheng Lun Zhi) [4]. Blood-stasis syndrome (BSS), which is characterized by impaired blood flow or stagnation, is one of the most prevalent TCM syndromes in metabolic diseases [5]. In TCM theory, metabolic disorder has been suggested to produce pathological substances, which constitute a pivotal factor in the etiology of BSS. Endothelial dysfunction is an early marker of ASCVD and has also been reported in BSS [6,7]. Moreover, BSS is associated with inflammation response [8], dyslipidemia, abnormal coagulation function, and fibrinolysis [9]. However, these pathologic changes have not been found in other TCM syndromes of T2DM. Consequently, among all TCM syndromes, BSS shows the closest relationship with the occurrence of ASCVD (also including other vascular complications) and vasculopathy. We hypothesize that specific metabolic changes may play a key role in this pathological process.

Metabolomics has gained widespread recognition as a highly sensitive method for molecular-level evaluation of the phenotype, positioning it at the forefront of biomarker and mechanistic evaluations of pathophysiological processes. It is particularly useful for identifying distinct biological characteristics among different subtypes, thereby advancing precision medicine [10]. Moreover, metabolomics has been extensively employed in research on T2DM [11] and TCM syndrome differentiation [12]. The untargeted metabolomics approach allows comprehensive coverage, facilitating extensive detection of substances in preliminary investigations and effectively characterizing the principal metabolic features of individuals.

As an emerging analytical method, pseudotargeted lipidomics integrates untargeted and targeted analyses and allows high-coverage and high-performance quantitative lipid analysis [13]. Moreover, it has been successfully employed in the discovery of differentially expressed serum lipids associated with diabetes [14]. Drawing from a thorough review of the literature and databases such as Lipid MAPS and LipidBlast, this study employs a high-throughput quantitative lipidomics method based on high-performance liquid chromatography-triple quadrupole mass spectrometry (HPLC-TQMS) for analysis of T2DM BSS. In this approach, quantitative analysis is enhanced using 74 isotope internal standards, offering exceptional sensitivity, stability, and reliability. This approach is especially suitable for serum sample analysis, enabling comprehensive lipid profiling in T2DM BSS.

Utilizing metabolomics and pseudotargeted lipidomics as the primary methodology, this study aimed to achieve several objectives: (1) to provide a comprehensive overview of the general metabolic characteristics of T2DM BSS; (2) to investigate the specific metabolites of T2DM BSS, using patients with non-blood-stasis syndrome (nBSS) and Healthy control (HC) as control groups; and (3) to provide a basis for future metabolite screening by combining the ROC curves of discovery cohort and validation cohorts as well as the MS/MS spectra of metabolites and initially screening the metabolites that differentiated T2DM BSS from the other two groups. These results allowed an initial exploration of BSS in T2DM from a microscopic perspective and identified the specific metabolites of BSS in T2DM from the perspective of combining disease and syndrome, thus providing a basis and reference for the future objective development of TCM syndrome differentiation.

2. Materials and methods

2.1. Clinical cohort

From October 2021 to November 2021, a total of 1189 residents in the Haidian district of Beijing were surveyed, and data collection was completed in January 2022. Ultimately 120 participants who met the inclusion and exclusion criteria were recruited, including 30 T2DM blood-stasis syndrome patients (BSS), 60 of T2DM non-blood-stasis syndrome patients (nBSS) and 30 of healthy control participants (HC). It is worth noting that according to the population proportion, there were more nBSS cases than BSS cases. Moreover, the differences in symptoms and metabolism within the nBSS group may be greater. To characterize the metabolic features of nBSS as comprehensively as possible, we expanded the sample size for this group. They were randomly divided into the discovery cohort (a total of 90, including 20 BSS, 50 nBSS, and 20 HC) and the validation cohort (a total of 30, including 10 BSS, 10 nBSS, and 10 HC), and their blood samples were collected for metabolic study. 21 of the above participants were selected for the psuedotargeted lipidomics (including 7 BSS, 7 nBSS, and 7 HC).

The diagnosis of T2DM was based on *Guideline for the prevention and treatment of type 2 diabetes mellitus in China* (*2020 edition*) [15]

and the BSS in T2DM diagnosis was based on *Guiding Principle of Clinical Research on New Drugs of Traditional Chinese Medicine* [5]. Participants were eligible if they had independent clinical diagnosis of Blood-stasis syndrome in T2DM (Table 1) by three senior TCM chief physicians who assessed the patients separately, and a patient is only included in the study when diagnosed with BSS by all three doctors. The exclusion criteria were as follows: age < 40 or > 85 years, acute complications including diabetic ketoacidosis, cardio-cerebral vascular diseases, severe liver and kidney dysfunction, hematological system diseases, malignancy or other terminal illness, major neuropsychiatric disorders, alcohol abuse and drug dependence, pregnant and lactating women, unable to cooperate in completing the collection of medical history and TCM syndrome sheets, have participated in other drug clinical trials within 3 months, incomplete information. Healthy individuals without diabetes, cardiovascular disease, stroke, hyperlipidemia, and other medical histories with complete data were screened as the HC group. The study followed the ethical principles of human medical research in the Declaration of Helsinki.

The research protocol was approved by the Ethics Committee of Xiyuan Hospital, China Academy of Chinese Medical Sciences (No. 2021XLA001-1), and written informed consent was obtained from each subject.

2.2. Sample collection and clinical measures

The researchers collected information of demographic, clinical and TCM information.

A 5 mL fasting morning blood sample was collected from the median cubital vein and placed in a precooling EDTA (Ethylene diamine tetraacetic acid) anticoagulation tube. Blood samples were centrifuged at 1530g at 4 °C for 10 min after blood collection. The separated plasma samples were put into liquid nitrogen and transferred to −80 °C before further use. No repeated freezing and thawing occurred before sample processing to avoid potential degradation risks of metabolites. Measurements of body mass index (BMI), systolic blood pressure (SBP), and diastolic blood pressure (DBP) were recorded. Fasting blood glucose (FPG), Glycosylated hemoglobin (HbA1c), Homocysteine (Hcy), Triglyceride (TG), Total cholesterol (TC), low-density lipoprotein cholesterol (LDL-C), and High-density lipoprotein cholesterol (HDL-C) were measured immediately.

2.3. Sample preparation

100 μL of serum sample was added to a 1.5 mL Eppendorf tube with 20 μL of L-2-chlorophenylalanine (0.6 mg/mL) dissolved in methanol as internal standard, and the tube was vortexed for 10s. Subsequently, 300 μL of an ice-cold mixture of methanol and acetonitrile (2/1, vol/vol) was added, the mixtures were vortexed for 1 min, and the whole samples were extracted by ultrasonic for 10 min in an ice-water bath, stored at −20 °C for 30 min. The extract was centrifuged at 4 °C(15620g) for 10min. 200 μL of supernatant in a Liquid chromatography-mass spectrometry (LC-MS) glass vial was dried in a freeze concentration centrifugal dryer. 300 μL mixture of methanol and water (1/4, vol/vol) was added to each sample, samples vortexed for 30s, extracted by ultrasonic for 3 min in an ice-water bath, then placed at −20 °C for 2h. Samples were centrifuged at 4 °C (15620g) for 10 min. The supernatants(150 μL) from each tube were collected using crystal syringes, filtered through 0.22 μm microfilters, and transferred to LC vials. The vials were stored at −80 °C until LC-MS analysis.

Lipids were extracted from 100 μL serum using 300 μL chloroform: methanol (2:1, v/v) contained known amounts of isotope-labeled internal mix standards, vortex for 30s and ultrasonic extraction for 10min, then holding 30min at −20 °C and transfer chloroform layers about 200 μL into a centrifuge tube after centrifugation 10min at 15620g and 4 °C. The residue was reextracted at the same condition above. Then combine the chloroform layers and lyophilize in a centrifugal vacuum evaporator at 4 °C. Finally,

Table 1
Inclusion criteria, exclusion criteria and diagnostic criteria for BSS.

Inclusion Criteria	Meeting the diagnostic criteria for T2DM and BSS, Signing of the informed consent form.
Exclusion Criteria	Age < 40 or > 85 years, acute complications including diabetic ketoacidosis, cardio-cerebral vascular diseases, severe liver and kidney dysfunction, hematological system diseases, malignancy or other terminal illness, major neuropsychiatric disorders, alcohol abuse and drug dependence, pregnant and lactating women, unable to cooperate in completing the collection of medical history and TCM syndrome sheets, have participated in other drug clinical trials within 3 months, incomplete information.
Diagnostic criteria for BSS	**Primary symptoms**: Pain in the chest
	Pain in the hypochondrium
	Pain in the fixed part
	Pricking pain
	Numbness of limbs
	Nocturnal pain
	Secondary symptoms: Xeroderma
	Dark purple lip
	Facial ecchymosis
	Amnesia and palpitation
	Vexation and insomnia
	Tongue and pulse: Dark purple or dark red tongue or with petechia or ecchymosis, sublingual vein cyanosis; wiry, sunken, or unsmooth pulse
	Patients who have at least two of the primary symptoms or three of the secondary symptoms can be diagnosed as showing blood-stasis syndrome

samples were reconstituted in isopropanol: methanol (1:1, v/v) vortex for 30s, ultrasonic extraction for 3min and centrifuge for 10min at 15620g and 4 °C and stored at −20 °C prior to LC-MS analysis.

2.4. Liquid chromatography-mass spectrometry based untargeted metabolomics

Quality-control (QC) samples were prepared by mixing aliquots of all samples to be a pooled sample. ACQUITY UPLC I-Class system (Waters Corporation, Milford, USA) coupled with VION IMS QTOF Mass spectrometer (Waters Corporation, Milford, USA) was used to analyze the metabolic profiling in both ESI positive and ESI negative ion modes. An ACQUITY UPLC HSS T3 column (1.8 μm, 2.1 × 100 mm) was employed in both positive and negative modes. Water and acetonitrile/Methanol 2/3(v/v), both containing 0.1 % formic acid were used as mobile phases A and B, respectively. Linear gradient: 0min, 1%B; 1min, 30%B; 2.5min, 60 % B; 6.5min, 90 % B; 8.5min, 100 % B; 10.7min, 100%B; 10.8min, 1 % B and 13min, 1 % B. The flow rate was 0.35 mL/min and column temperature was 45 °C. All the samples were kept at 4 °C during the analysis. The injection volume was 1 μL.

2.5. Liquid chromatography-tandem mass spectrometry based pseudotargeted lipidomics

The LC system utilized an ExionLC™ System comprising a binary high-pressure mixing gradient pump with a degasser, a thermostated autosampler, and a column oven. The MS was QTRAP® 6500+ (Sciex, USA) equipped with an IonDrive™ Turbo V source. Optimization conditions were as follows: autosampler temperature set at 10 °C, sample injection volume of 5 μL. Eluents were 0.1 % formic acid and 10 mM ammonium formate in 6:4 acetonitrile/water (eluent A) and 1:9 acetonitrile/methanol with 0.1 % formic acid and 10 mM ammonium formate (eluent B). Flow rate was 0.35 mL/min. A 20-min elution gradient with a UPLC HSS T3 column was performed: 0 % B initially for 1.5 min, linearly changed to 55 % B at 5 min, 60 % B at 10 min, 70 % at 13 min, 90 % at 15 min, increased to 100 % in the next 1 min and maintained for 2 min. Then recovered initial conditions for 2 min for column conditioning. The MS method was in negative/positive-ion mode with time-scheduled MRM. Source condition: curtain gas 35 psi, CAD medium, IS -4500V/+5500V, Gas1 and Gas2 40 psi and 45 psi respectively. 15 kinds of glycerophospholipids, glycerolipids, and sphingolipids isotope-labeled internal mix standards were from Avanti Polar Lipids. Palmitic acid-16,16,16-d3, Stearic acid-18,18,18-d3, and different Acyl carnitine-d3 were from Sigma-Aldrich. HPLC grade organic solvents and water for sample and mobile phase preparations were from Fisher Scientific. All stock solutions were stored at −20 °C.

2.6. Data processing

The original LC-MS data were processed by Progenesis QI V2.3 software for baseline filtering, peak identification, integration, retention time correction, peak alignment, and normalization. Parameters of 5 ppm precursor tolerance, 10 ppm product tolerance, and 5 % production threshold were applied. Compound identification was based on M/z, secondary fragments, and isotopic distribution using HMDB, Lipidmaps (V2.3), Metlin, EMDB, PMDB, and self-built databases for qualitative analysis. Extracted data were further processed by removing peaks with missing values in >50 % of groups, replacing zeros with half the minimum value, and screening according to qualitative results. Compounds with scores <36 were removed. A data matrix from positive and negative ion data was combined and imported into R version 4.2.2 for OPLS-DA to distinguish group-differentiating metabolites. 7-fold cross-validation [16] and 200 Response Permutation Testing (RPT) were used to evaluate the quality of the model. Variable Importance of Projection (VIP) values from the OPLS-DA model ranked variable contributions. The metabolic pathway enrichment analysis was

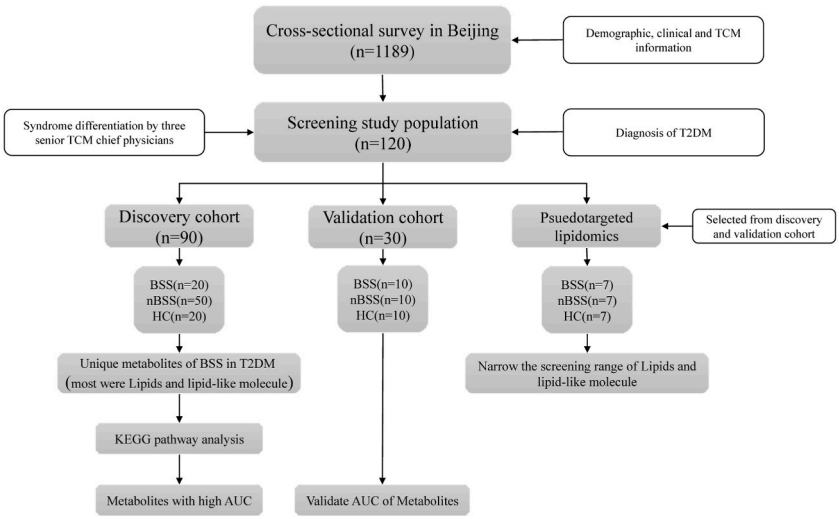

Fig. 1. The flowchart of the strategy of the study.

evaluated via MetaboAnalyst (www.metaboanalyst.ca) using the Kyoto Encyclopedia of Genes and Genomes (KEGG) database (https://www.kegg.jp/). The venn diagram was produced by Sangerbox 3.0 (http://sangerbox.com/). The R statistical package was used to generate receiver operating characteristics (ROC) curves and area under the curve (AUC).

2.7. Statistical analysis

Comparisons were performed with T-test, Wilcoxon–Mann–Whitney, and one-way ANOVA as appropriate. Non-parametric tests were used for comparing ordinal or non-HC variables. A two-tailed Student's T-test was further used to verify whether the metabolites of difference between groups were significant. Unique metabolites were selected with VIP >1.0. Significance was defined as $P < 0.05$.

3. Results

3.1. Demographic and clinical characteristics of patients

The workflow of the study is illustrated in Fig. 1. The general clinical characteristics of BSS, nBSS, and HC are presented in Table 2. There were no significant differences in age, gender, BMI, waistline, DBP, TG, TC HDL-C, LDL-C between BSS, nBSS, and HC. T2DM groups (BSS and nBSS) showed higher SBP, FPG, and HbA1c than HC. Meanwhile, BSS had significantly higher levels of Hcy.

3.2. Untargeted metabolomics analysis of serum samples

3.2.1. Metabolic profiles of BSS group, nBSS group, and HC group

To identify the serum metabolome features of BSS and nBSS, untargeted metabolome profiles were generated on 90 fasting serum samples by LC-MS, the representative BSS, nBSS, and HC are shown in Supplementary Figs. S1A and S1B. There were differences in metabolite profiles in the positive and negative ion modes in the three groups.

3.2.2. Multivariate statistical analysis of metabolites in BSS, nBSS, and HC groups

All the QC samples clustered closely, verifying the reliability of the present study, and verifying the reliability of the present study without overfitting the model (Supplementary Figs. S1C and S1D). It was demonstrated the three groups were visually distinguished in the 3-dimensional spatial distribution (Fig. 2A,B,2C), indicating that the metabolism pattern was changed among the three groups. The results of R^2X, R^2Y, $R^{2,}$ and Q^2 indicated that the prediction model is not over-fitted.

Table 2
General clinical characteristics of the BSS, nBSS, and HC groups.

Covariate	BSS(n = 20)	Discovery cohort(n = 90)	HC(n = 20)	*P* value	BSS(n = 10)	Validation cohort(n = 30)	HC(n = 10)	*P* value
		nBSS(n = 50)				nBSS(n = 10)		
Age(years)	63.20 ± 8.24	65.94 ± 5.22	64.2 ± 6.20	0.2	71.6 ± 11.68	65.2 ± 7.91	73.3 ± 7.99	0.14
male,n (%)	9 (45)	25 (50)	10 (50)	0.93	5 (50)	5 (50)	5 (50)	1
BMI (kg/m^2)	24.75 ± 3.94	24.99 ± 3.46	24.31 ± 3.19	0.76	23.80 ± 2.54	23.47 ± 3.76	22.34 ± 3.13	0.57
Waistline(cm)	90.2 ± 12.32	86.36 ± 10.90	86.95 ± 7.98	0.39	88.20 ± 9.38	86.9 ± 9.78	63.00 ± 4.94	0.04
SBP (mmHg)	137.65 ± 11.87	142.94 ± 22.62	123.75 ± 8.64	< 0.01*#	153.90 ± 22.05	135.00 ± 11.96	123.1 ± 11.27	< 0.01*#
DBP (mmHg)	83.95 ± 9.68	81.22 ± 10.83	80.20 ± 7.30	0.45	83.3 ± 12.67	76.60 ± 9.92	80.00 ± 6.24	0.34
FPG (mmol/L)	8.06 ± 2.58	7.88 ± 3.10	4.81 ± 1.50	< 0.01*#	8.08 ± 2.98	7.91 ± 2.94	5.28 ± 1.07	< 0.03*#
HbA1c(%)	7.24 ± 1.98	6.70 ± 1.36	5.34 ± 1.32	< 0.01*#	6.13 ± 1.03	7.32 ± 1.31	5.20 ± 0.39	< 0.01*#
TG (mmol/L)	1.58 ± 0.66	1.56 ± 0.81	1.35 ± 0.71	0.54	1.32 ± 0.84	1,71 ± 0.88	1.36 ± 0.82	0.53
TC (mmol/L)	3.94 ± 0.98	4.39 ± 1.07	4.42 ± 1.02	0.22	4.24 ± 1.07	4.23 ± 1.12	4.95 ± 2.00	0.46
LDL-C(mmol/L)	2.16 ± 0.66	2.40 ± 0.94	2.45 ± 0.75	0.49	2.37 ± 0.81	2.27 ± 1.15	2.23 ± 0.44	0.94
HDL-C(mmol/L)	1.25 ± 0.27	1.39 ± 0.30	1.41 ± 0.31	0.16	1.42 ± 0.34	1.22 ± 0.29	1.62 ± 0.58	0.13
Hcy(μmol/L)	22.21 ± 10.69	13.95 ± 5.15	14.01 ± 3.85	< 0.01* $	22.27 ± 14.29	11.85 ± 3.21	12.55 ± 3.08	< 0.05* $

BSS, blood-stasis syndrome; nBSS, non-blood-stasis syndrome; HC, healthy control; BMI body mass index, SBP systolic blood pressure, DBP diastolic blood pressure, FPG fasting blood-glucose, HbA1c glycosylated hemoglobin, TG triglyceride, TC total cholesterol, LDL-C low-density lipoprotein, HDL-C high-density lipoprotein, Hcy homocysteine. *P < 0.05 BSS vs. HC. #P < 0.05 nBSS vs. HC. $P < 0.05 BSS vs. nBSS.

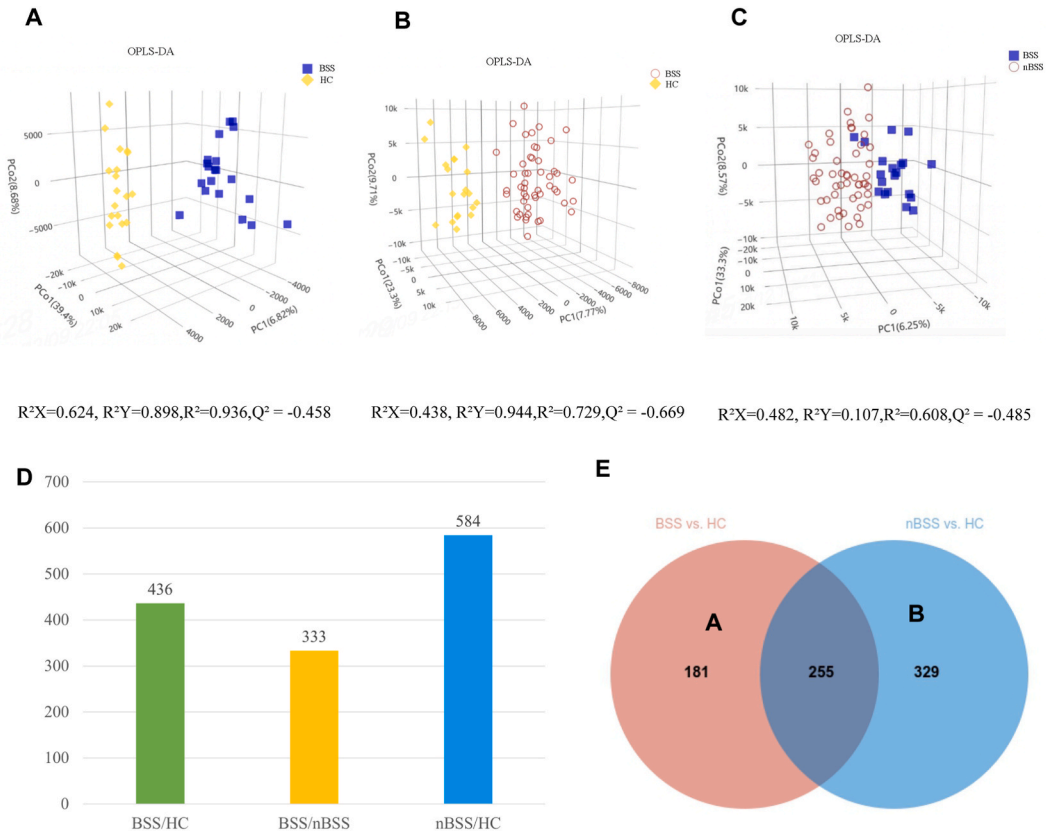

Fig. 2. The 3-dimensional orthogonal projection to latent structure-discriminant analysis (3D OPLS-DA) score plots and differential metabolites. (A) BSS vs. HC. (B) nBSS vs. HC. (C) BSS vs. nBSS. (D) Bar chart illustrating the number of differential metabolites between groups. (E) Overlaps of differential metabolites of BSS vs. HC and nBSS vs. HC.

3.2.3. Unique metabolites of T2DM BSS

Based on the significant changes in the comparisons among the three groups, multivariate and univariate statistical significance criteria were applied to determine differential metabolites (VIP >1, *P* value < 0.05), and ultimately, 765 differential metabolites were found (Fig. 2D). To visualize the relationship between samples and the different metabolite expressions in groups, hierarchical clustering of all significantly different metabolite expressions was performed, heatmaps were used to show the expression of metabolites in different groups, and volcano plots were used to show the up- and down-regulated of metabolites. In the comparison between the BSS and HC, 436 differential metabolites were identified, including 226 positive ions and 210 negative ions (Supplementary Fig. S2A). In the comparison between the nBSS and HC, 584 differential metabolites were identified, including 360 positive ions and 224 negative ions (Supplementary Fig. S2B). In the comparison between the BSS and nBSS, 333 differential metabolites were identified, including 210 positive ions and 123 negative ions (Supplementary Fig. S2C).

To identify unique metabolites of T2DM BSS, it is necessary to exclude metabolites that may be commonly associated with T2DM. The differential metabolites between BSS and HC (A) encompassed T2DM-related and BSS-related metabolites. Similarly, the differential metabolites between nBSS and HC (B) included T2DM-related and nBSS-related metabolites. Therefore, A-(A∩B) represented the exclusive set of metabolites specific to BSS, and the Venn diagram was used to visualize the above process (Fig. 2E). Initially, a total of 181 metabolites were identified, and for more precise screening, we set the exclusion criteria VIP >1.5, *P* value < 0.05, finally 81 metabolites were selected (Supplementary Table S1). Meanwhile, to distinguish BSS and nBSS in T2DM patients, the differential metabolites between the two groups were also selected (VIP >1.5, *P* value < 0.05), eventually we screened out 2 metabolites that could be used to distinguish BSS and nBSS (Supplementary Table S2). The MS/MS spectra of all the above metabolites are shown in Supplementary File 3. Heatmap (Fig. 3A) showed the relative intensity distribution of the unique metabolites of 3 groups, the above metabolites belonged to Glycerophospholipids, Fatty Acyls, Carboxylic acids and derivatives, Diazines, Lactones, Organooxygen compounds, Phenol ethers, Phenols Polyketides, Prenol lipid, Pyridines and derivatives, Sphingolipids, Steroids and steroid derivatives, Thiol. Glycerophospholipids and Fatty Acyls were the most abundant class. The Pearson correlation coefficient was employed to investigate the association between unique metabolites of BSS using a heatmap, wherein positive correlations were depicted in red and negative correlations in blue. A majority of the metabolites exhibited positive associations (Supplementary Fig. S2D).

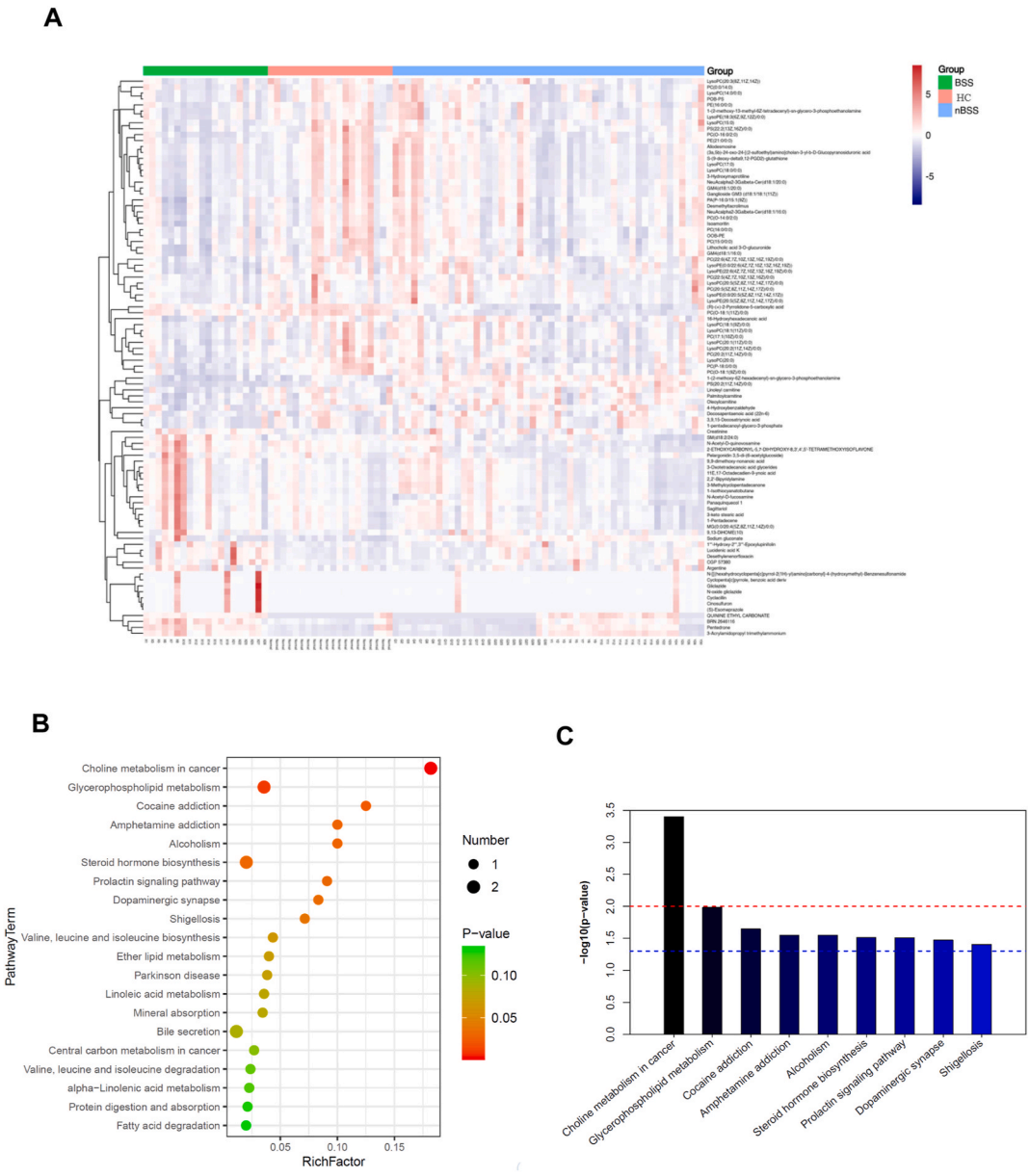

Fig. 3. Differential Metabolites between groups and pathway enrichment. (A) Heatmap of 81 differential metabolites of BSS. (B) The enrichment of the top 20 metabolic pathways according to the identified distinguished metabolites in BSS by MetaboAnalyst. (C) 9 metabolic pathways of the top 20 metabolic pathways.

3.2.4. Pathway enrichment of unique metabolites in T2DM BSS

A functional pathway analysis was performed to identify the metabolic pathways that were disrupted in BSS patients. Based on Metaboanalyst enrichment analysis, the top 20 enriched pathways (Fig. 3B) were revealed and 9 of them had $p < 0.05$ (Fig. 3C), including choline metabolism in cancer, glycerophospholipid metabolism (Supplementary Fig. 5), Cocaine addiction, Amphetamine addiction, Alcoholism, Steroid hormone biosynthesis, Prolactin signaling pathway, Dopaminergic synapse and Shigellosis.

3.2.5. Analysis of the diagnostic Power of unique metabolites

To determine whether the metabolite modules can be regarded as identification biomarkers for distinguishing BSS from HC and nBSS, ROC curves were constructed to classify differences, and receiver operating characteristic (ROC) curves were used to test the 81 metabolites and metabolites with the highest AUC were screened out. The results showed that LysoPC (20:5(5Z,8Z,11Z,14Z,17Z)/0:0) had the greatest impact to distinguish BSS and HC ($P = 0.0288$) (Fig. 4A,C) and LysoPC (15:0) had the greatest impact to distinguish BSS and nBSS ($P = 0.0126$) (Fig. 4B and D).

3.2.6. Validation of diagnostic Power of unique metabolites

To reduce the bias caused by samples, we enrolled another independent validation cohort that met the same inclusion and exclusion criteria as the discovery phase, general characteristics of the validation cohort are shown in Table 1. Consistent with the results of the discovery cohort, LysoPC (20:5(5Z,8Z,11Z,14Z,17Z)/0:0) had the greatest impact on distinguishing BSS and HC (Fig. 4E), LysoPC (15:0) had the greatest impact to distinguish BSS and nBSS (Fig. 4F) in validation cohort, and the trend of the above metabolites was the same as discovery cohort.

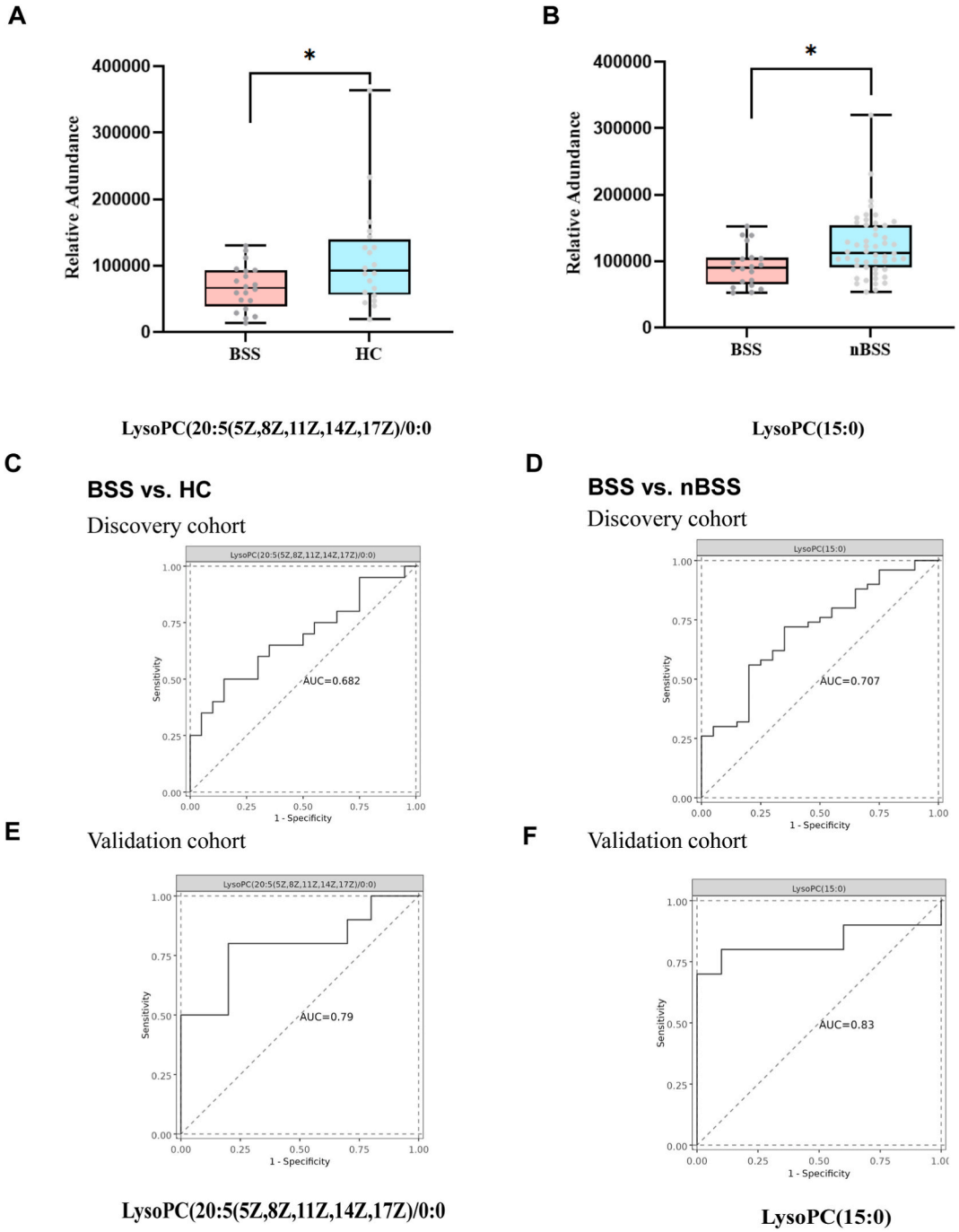

Fig. 4. Diagnostic value of selected metabolites. (A) Box plots of LysoPC (20:5(5Z,8Z,11Z,14Z,17Z)/0:0) (B) Box plots of LysoPC (15:0). (C) ROC of LysoPC (20:5(5Z,8Z,11Z,14Z,17Z)/0:0) to distinguish BSS and HC in the discovery cohort. (D) ROC of LysoPC(15:0) to distinguish BSS and nBSS in the discovery cohort. (E) ROC of LysoPC (20:5(5Z,8Z,11Z,14Z,17Z)/0:0) to distinguish BSS and HC in the validation cohort. (F) ROC of LysoPC (15:0) to distinguish BSS and nBSS in the validation cohort.

3.3. Pseudotargeted lipidomics analysis of serum samples

Untargeted metabolomics revealed that most of the differential metabolites of BSS were Lipids and lipid-like molecules, so 21 serum samples were selected for pseudotargeted lipidomics Analysis. Pseudotargeted lipidomics profiles of the representative BSS, nBSS, and HC are shown in Supplementary Fig. S3. All the QC samples clustered closely, verifying the reliability of the present study without overfitting of the model (Supplementary Figs. S4A and S4B).

Pseudotargeted lipidomics was also employed to identify metabolites that distinguish BSS, nBSS and HC groups. The metabolic profile differences between the groups in the discovery cohort were visualized using OPLS-DA (Fig. 5A,B,5C), it was demonstrated the three groups were visually distinguished, and the results of R^2X, R^2Y, R^2 and Q^2 indicated that the prediction model is not over-fitted. Volcano plots were used to show the difference of metabolites in 3 groups (Supplementary Fig. S4C).

In the comparison between BSS and HC, a total of 8 lipids were identified; in the comparison between nBSS and HC, a total of 24 lipids were identified; and in the comparison between BSS and nBSS, a total of 7 lipids were identified (Fig. 5D,E,5F). Z-score plots are shown in Fig. 6A,B,6C. The top 5 lipids with the highest VIP value for each comparison are listed in Table 3. Glycerolipids and Glycerophospholipids were the most abundant class and mainly included phosphatidylcholine (PC), diacylglycerol (DAG), and triacylglycerol (TAG).

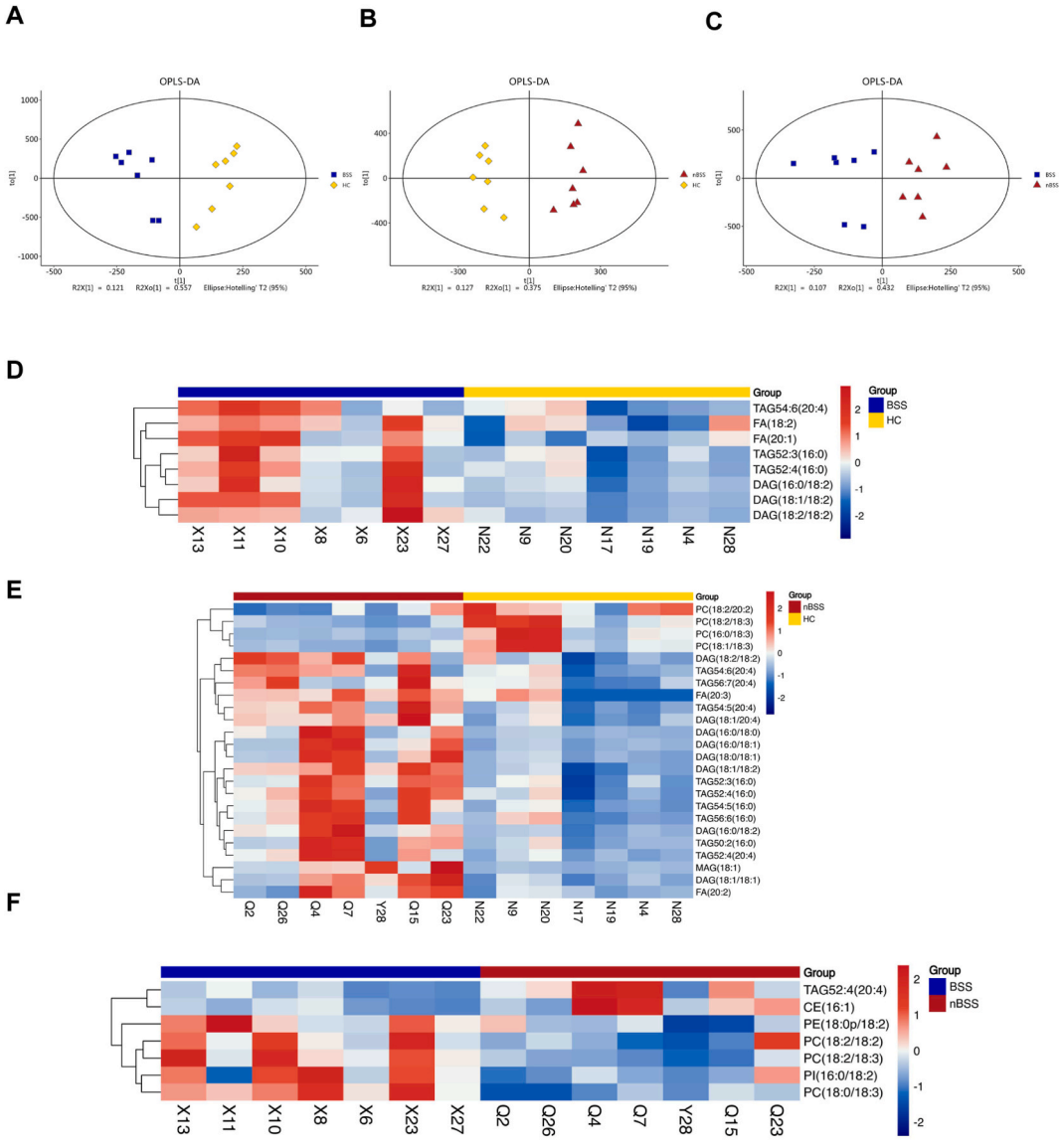

Fig. 5. Analysis of serum pseudotargeted lipidomics. (A) (B) (C) Orthogonal Partial Least-Squares-Discriminant Analysis (OPLS-DA) of BSS vs. HC, nBSS vs. HC and BSS vs. nBSS. (D) Heatmaps of differential metabolites of BSS vs. HC. (E) Heatmaps of differential metabolites of nBSS vs. HC. (F) Heatmaps of differential metabolites of BSS vs. nBSS.

To identify distinctive lipids of T2DM BSS, it is necessary to exclude lipids that may be commonly associated with T2DM. Using the same approach as untargeted metabolomics used in 3.2.3, distinctive lipids of T2DM BSS were also identified (Fig. 6D). The findings revealed that FA (18:2) and FA (20:1) were distinctive lipids observed in T2DM BSS patients, exhibiting upregulation (Fig. 6E,F).

4. Discussion

T2DM is a metabolic disorder disease, and the cardiovascular endothelial cell injury caused by the abnormal metabolic state may lead to diabetic vascular diseases. Among all TCM syndromes of T2DM, only BSS shows a strong association with vascular injury. At present, diagnosis is based on macroscopic information, The microcosmic metabolism of BSS in T2DM (T2DM BSS) is not clear enough, making precise syndrome differentiation and targeted treatment a significant challenge. This study employed a combination of untargeted metabolomics and pseudotargeted lipidomics to delineate the general metabolic and lipid profiles of T2DM BSS. Due to the advantages of comprehensiveness, sensitivity, excellent reproducibility, and wide application of LC-MS, we selected it as the research method. Consistent clinical baseline statuses were used for screening and comparison across all populations, as illustrated in Fig. 1.

We confirmed that patients with T2DM BSS exhibited significantly distinct metabolite profiles in comparison with the nBSS and HC groups (Fig. 2). This was confirmed by the significant expression differences between the three groups of metabolites in Fig. 3A. The

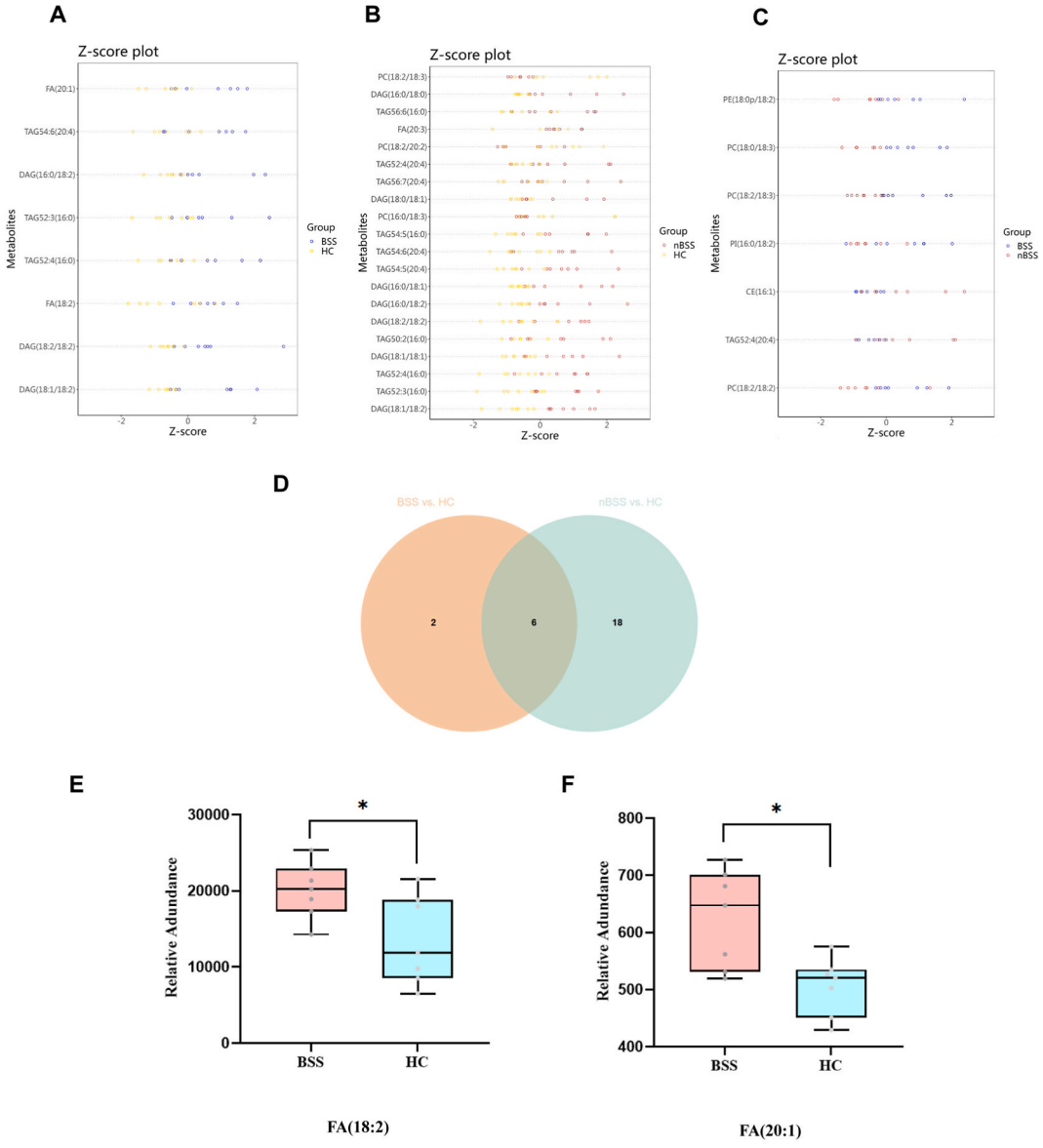

Fig. 6. Z-score plots and unique lipids of T2DM BSS. (A) Z-score plots of BSS vs. HC. (B) Z-score plots of nBSS vs. HC. (C) Z-score plots of BSS vs. nBSS. (D) Overlaps of lipids of BSS vs. HC and nBSS vs. HC. (E) Box plots of 2 selected unique lipids of T2DM BSS.

Table 3
Differential lipids identified by Pseudotargeted Lipidomics.

Group	Metabolite	VIP	*P-value*	FC	Class	Ion mode	KEGG
	DAG (18:1/18:2)	8.29	0.0061	2.34	Glycerolipids	pos	–
	DAG (18:2/18:2)	6.39	0.0100	2.37	Glycerolipids	pos	C00165
BSS vs **HC**	FA (18:2)	5.08	0.0290	1.48	Fatty acyls	neg	–
	TAG52:4(16:0)	5.08	0.027	1.59	Glycerolipids	Pos	–
	FA(20:1)	1.46	0.01	1.23	Fatty acyls	neg	–
	DAG (18:1/18:2)	6.34	0.0001	1.86	Glycerolipids	pos	–
	TAG52:3(16:0)	5.35	0.0054	1.48	Glycerolipids	pos	–
nBSS vs **HC**	TAG52:4(16:0)	5.08	0.0058	1.55	Glycerolipids	pos	–
	DAG (18:1/18:1)	4.90	0.007	2.36	Glycerolipids	pos	–
	TAG50:2(16:0)	4.69	0.039	1.87	Glycerolipids	pos	–
	PC (18:2/18:2)	6.85	0.0468	1.73	Glycerophospholipids	neg	C00157
	TAG52:4(20:4)	1.45	0.0355	0.39	Glycerolipids	pos	–
BSS vs **nBSS**	CE (16:1)	1.35	0.0401	0.32	Sterol Lipids	pos	–
	PI (16:0/18:2)	1.34	0.0453	1.43	Glycerophospholipids	neg	C00626
	PC (18:2/18:3)	1.34	0.0024	3.17	Glycerophospholipids	neg	C00157

BSS, blood-stasis syndrome; nBSS, non-blood-stasis syndrome; HC, healthy control.

alterations in the metabolome reflected biochemical changes related to blood stasis. Notably, lipids and lipid-like molecules constituted the largest groups of differentially expressed metabolites, accounting for 49 types (60.5 %) between BSS and HC, and 94 types (61.4 %) between BSS and nBSS, which is consistent with previous reports [17] **(**Supplementary Table S1). Pseudotargeted lipidomics results further indicated that lipid disorders were the primary form of dysregulation observed in T2DM BSS (Table 3). Lipids are known to be the most diverse class of small molecule compounds in eukaryotic organisms, serving structural roles while participating in cellular transport, energy storage, and cellular signaling [18]. Moreover, dysfunction of lipid metabolism is closely linked to inflammation and oxidative stress, both of which play crucial roles in the initiation and progression of atherosclerosis [19]. Plasma lipids have been implicated in the development of diabetic complications such as cardiovascular disease and nephropathy; furthermore, local dysregulation of lipid metabolism has been shown to contribute to rapid progression of kidney disease [20]. A prospective study revealed that plasma lipid species could enhance the prediction accuracy for cardiovascular events among individuals with diabetes mellitus [21].

Consistent with previous reports [22], our study identified significant alterations in glycerophospholipids, including phosphatidylcholines (PCs), phosphatidylethanolamines (PEs), lysophosphatidylcholine (LPCs), and lysophosphatidylethanolamine (LPEs), in T2DM BSS **(**Supplementary Table S1). In addition, we observed that LysoPC (20:5(5Z,8Z,11Z,14Z,17Z)/0:0) and LysoPC (15:0) showed the strongest ability to distinguish BSS, and this result was verified in the validation cohort (Fig. 4). Alterations in phospholipid concentration indicate alterations in cell membrane composition and permeability, which can influence normal cellular physiological functions [23]. Glycerophospholipids, as the primary lipid constituents of cell membranes that directly influence cellular physiological functions, serve as crucial biological indicators for assessing lipid metabolism disorders [24]. As a novel class of inflammatory lipids, glycerophospholipids play important roles in atherosclerosis, diabetes, cancer, inflammation, and blood lipid disorders [25]. Recent studies have reported notable differences in glycerophospholipids among TCM syndromes [26]. Moreover, studies have shown that herbs regulated glycerophospholipid metabolism to prevent and alleviate blood stasis, alleviating cold - stagnation and blood-stasis primary dysmenorrhea and protecting renal function in diabetic mice [27]. Our findings also revealed significant downregulation of PCs, PEs, LPCs, and LPEs in patients with T2DM BSS. To our knowledge, PCs and PEs account for more than 50 % of the composition of glycerophospholipid; changes in the PC/PE molar ratio affect energy production; and their content has been implicated in metabolic disorders [28]. Recent studies have shown that PCs and PEs are negatively correlated with AS severity and myocardial markers [29], and significantly decreased levels of LPCs may be associated with decreased cognitive speed and obesity [30]. These observations suggest that patients with T2DM BSS may face greater disruptions in energy production, leading to increased membrane or cellular damage. This could potentially result in a higher incidence of complications, especially cardiovascular diseases, than in other T2DM patients.

Marked disorders of FAs and sphingolipids were observed in patients with T2DM BSS **(**Supplementary Table S1). Furthermore, a pseudotargeted lipidomics approach exclusively showed upregulated levels of FA (18:2) and FA (20:1) lipids (Fig. 6E,F). Sphingolipids serve as crucial signaling molecules involved in various cellular functions and play significant roles as regulators and mediators of inflammatory responses [31]. Among sphingolipids, SM(d18:2/24:0) was found to be upregulated in T2DM BSS. Sphingomyelin (SM) is the second most abundant phospholipid component and the major sphingolipid in high-density lipoprotein (HDL) [32], and can be used to distinguish patients with diabetic nephropathy from healthy individuals [33]. Furthermore, fatty acid and sphingosine are constituents of ceramides, which are signaling molecules involved in the regulation of inflammation and insulin resistance related to obesity [34]. Diabetes, inflammation and obesity are associated with an increased incidence of atherothrombotic events [35]. Simultaneously, ceramides target specific enzymes that produce lipotoxic molecules, and according to the lipotoxicity hypothesis, oversupply of lipids to tissues not suited for fat storage leads to the accumulation of fat-derived molecules that impairs tissue function, thus causing damage to the cardiovascular and renal systems [36]. Ceramides have been of interest in studies on the development of diabetic complications because they are involved in the pathological processes of inflammation and lipotoxicity. Since they are regarded as potential early metabolic markers of progression to diabetes, ceramides have been associated with the risk of incident

major cardiovascular events [37]. In summary, the pronounced disorders of FAs and sphingolipids in patients with T2DM BSS indicate underlying pathological changes linked to inflammation and lipotoxicity. This may provide a basis for understanding the stronger connection between T2DM BSS and diabetic vascular complications, owing to more specific vascular impairment.

In the present study, in comparison with HC, patients with T2DM BSS showed significantly higher L-isoleucine (Supplementary Table S1), and higher homocysteine levels (Table 2). L-isoleucine belongs to the branched-chain amino acid, and decreased L-serine levels and increased levels of branched-chain amino acids are the most frequent alterations in plasma amino acid concentrations in T2DM; these alterations have been shown to lead to decreased synthesis of phospholipids, impaired homocysteine disposal, and increased levels of aromatic amino acids [38], which may explain the changing trends of phospholipids and homocysteine in the current study. Other studies have concluded that L-isoleucine is involved in maintaining immunity and regulating the inflammatory response [39]. Our results confirmed that increased L-isoleucine levels were accompanied by increased levels of Hcy in BSS, which was consistent with our expectations. The L-isoleucine disorders suggested that inflammation potentially contributes to the pathological mechanisms underlying T2DM BSS again.

The results of KEGG pathway analysis (Fig. 3B,C) indicated that the downregulation of phosphatidylcholine (PtdCho) and 1-acyl-glycerophosphocholine (1-acyl-GPC) primarily leads to dysregulation in glycerophospholipid metabolism and choline metabolism in cancer. The upregulation of pregnanediol and dehydroepiandrosterone contributes to disturbances in steroid hormone biosynthesis, while the downregulation of L-DOPA affects multiple pathways, including those related to cocaine addiction, amphetamine addiction, alcoholism, dopaminergic synapse, prolactin signaling pathway, and shigellosis. PtdCho, which was downregulated in BSS, is the most abundant phospholipid in mammalian cell membranes. In a catabolic pathway, PtdCho is broken down to 1-acyl-GPC and GPC, which is subsequently converted to free choline, thus completing the choline cycle [40]. Activated choline metabolism is characterized by increased levels of phosphocholine (PC), glycerophosphocholine (GPC) and total choline-containing compounds (tCho), which is a hallmark of carcinogenesis and tumor progression [41], while increased glycolytic activity is another metabolic features of cancer cells [42]. Steroid hormones play an essential role in regulating water and salt balance, metabolism and stress response, and in initiating and maintaining sexual differentiation and reproduction, and measurement of individual steroids levels has been routinely employed for the diagnosis of endocrine conditions [43]. The observed alterations in metabolic pathways indicate the altered physiological function in patients with T2DM BSS.

Based on a large sample population, with nBSS and HC as control groups, we excluded differential metabolites that may be common in T2DM. We discovered that glycerophospholipids were the main constituents of the core metabolites in T2DM BSS, while FA (18:2) and FA (20:1) were identified as differential lipids. Furthermore, our findings revealed significant dysregulation in glycerophospholipid metabolism and choline metabolism within cancer pathways as major metabolic disturbances associated with T2DM BSS. These metabolic changes are believed to contribute to inflammation, oxidative stress, and lipotoxicity which could potentially lead to the vascular damage–related pathological mechanisms of T2DM BSS. Furthermore, analyses of both the discovery and validation cohorts revealed LysoPC(20:5(5Z,8Z,11Z,14Z,17Z)/0:0) as a potential biomarker for distinguishing between individuals with BSS and HC; whereas LysoPC (15:0) showed promise for distinguishing between individuals with BSS and nBSS.

This study had several limitations that require consideration. First, the study population was recruited on the basis of stringent exclusion criteria and diagnostic guidelines. Consequently, our final sample consisted of only 120 individuals out of the 1189 residents screened, which limited the breadth of our data. Additionally, the study was subject to geographical constraints, which potentially influenced the broader applicability of our findings. Moreover, while pseudotargeted lipidomics was effectively utilized to investigate the lipid metabolism characteristics of T2DM BSS, due to financial constraints, the small sample size restricted further in-depth data analysis. Lastly, this study primarily focused on the metabolic profile of T2DM BSS. Future studies should, therefore, focus on a more targeted analysis of metabolites to enhance the precision of the results.

5. Conclusion

In conclusion, our results suggest that glycerophospholipids and FAs are associated with T2DM BSS. The presence of inflammation, oxidative stress, and lipotoxicity underlying these metabolic disorders may contribute to vascular damage, thereby explaining the close relationship between T2DM BSS and diabetic vascular complications. Additionally, LPCs have the greatest impact on distinguishing BSS. These results provide valuable mechanistic insights linked with the development of BSS in T2DM subjects.

CRediT authorship contribution statement

Li Liu: Writing – original draft, Visualization, Methodology, Investigation, Conceptualization. **Yuan-bin Liang:** Methodology. **Xiao-lin Liu:** Methodology. **Hong-qin Wang:** Writing – review & editing. **Yi-fei Qi:** Writing – review & editing. **Min Wang:** Visualization. **Bao-xin Chen:** Validation. **Qing-bing Zhou:** Supervision. **Wen-xin Tong:** Funding acquisition. **Ying Zhang:** Supervision, Funding acquisition.

Data availability statement

Data included in article/supp. material/referenced in article. The datasets used and/or analyzed during the current study available from the corresponding author on reasonable request.

Ethics approval and consent to participate

The study followed the ethical principles of human medical research in the Declaration of Helsinki. The research protocol was approved by the Ethics Committee of Xiyuan Hospital, China Academy of Chinese Medical Sciences (No. 2021XLA001-1), dated on January 7, 2021. Informed consent was obtained from each subject.

Funding

This study was supported by the National Key Research and Development Project of China (Grant No.2018YFC1704303) and Key Projects for Scientific and Technological Innovation of China Academy of Chinese Medical Sciences (Grant No.CI2021A01407, No. CI2021A01408).

Declaration of competing interest

The authors declare the following financial interests/personal relationships which may be considered as potential competing interests: Ying Zhang reports financial support was provided by Institute of Geriatric Medicine, Xiyuan Hospital, China Academy of Chinese Medical Sciences. If there are other authors, they declare that they have no known competing financial interests or personal relationships that could have appeared to influence the work reported in this paper.

Acknowledgments

Not applicable.

Appendix A. Supplementary data

Supplementary data to this article can be found online at https://doi.org/10.1016/j.heliyon.2024.e39554.

References

[1] American Diabetes Association Professional Practice Committee, 2, Classification and diagnosis of diabetes: standards of medical care in diabetes-2022, Diabetes Care 45 (2022) S17–S38, https://doi.org/10.2337/dc22-S002.
[2] R.H. Ritchie, E.D. Abel, Basic mechanisms of diabetic heart disease, Circ. Res. 126 (2020) 1501–1525, https://doi.org/10.1161/CIRCRESAHA.120.315913.
[3] S. Li, Z. Wu, W. Le, Traditional Chinese medicine for dementia, Alzheimers Dement 17 (2021) 1066–1071, https://doi.org/10.1002/alz.12258.
[4] M. Jiang, C. Lu, C. Zhang, J. Yang, Y. Tan, A. Lu, K. Chan, Syndrome differentiation in modern research of traditional Chinese medicine, J. Ethnopharmacol. 140 (2012) 634–642, https://doi.org/10.1016/j.jep.2012.01.033.
[5] X. Zheng, Guiding Principle of Clinical Research on New Drugs of Traditional Chinese Medicine, China Medical Science and Technology, Beijing, 2002.
[6] G.-H. Zheng, S.-Q. Xiong, H.-Y. Chen, L.-J. Mei, T. Wang, Association of platelet-activating factor receptor gene rs5938 (G/T) and rs313152 (T/C) polymorphisms with coronary heart disease and blood stasis syndrome in a Chinese Han population, Chin. J. Integr. Med. 23 (2017) 893–900, https://doi.org/10.1007/s11655-017-2802-4.
[7] Y.-H. Li, Q. Xu, W.-H. Xu, X.-H. Guo, S. Zhang, Y.-D. Chen, Mechanisms of protection against diabetes-induced impairment of endothelium-dependent vasorelaxation by Tanshinone IIA, Biochim. Biophys. Acta 1850 (2015) 813–823, https://doi.org/10.1016/j.bbagen.2015.01.007.
[8] C.-Y. Ma, J.-H. Liu, J.-X. Liu, D.-Z. Shi, Z.-Y. Xu, S.-P. Wang, M. Jia, F.-H. Zhao, Y.-R. Jiang, Q. Ma, H.-Y. Peng, Y. Lu, Z. Zheng, F.-X. Ren, Relationship between two blood stasis syndromes and inflammatory factors in patients with acute coronary syndrome, Chin. J. Integr. Med. 23 (2017) 845–849, https://doi.org/10.1007/s11655-016-2746-0.
[9] Q.-Q. Xin, X. Chen, R. Yuan, Y.-H. Yuan, J.-Q. Hui, Y. Miao, W.-H. Cong, K.-J. Chen, Correlation of platelet and coagulation function with blood stasis syndrome in coronary heart disease: a systematic review and meta-analysis, Chin. J. Integr. Med. 27 (2021) 858–866, https://doi.org/10.1007/s11655-021-2871-2.
[10] I.R. König, O. Fuchs, G. Hansen, E. von Mutius, M.V. Kopp, What is precision medicine? Eur. Respir. J. 50 (2017) 1700391 https://doi.org/10.1183/13993003.00391-2017.
[11] Q. Yang, A. Vijayakumar, B.B. Kahn, Metabolites as regulators of insulin sensitivity and metabolism, Nat. Rev. Mol. Cell Biol. 19 (2018) 654–672, https://doi.org/10.1038/s41580-018-0044-8.
[12] N. Jiang, H. Liu, S. Li, W. Zhou, Y. Zhang, Q. Zhang, X. Yan, An integrated metabonomic and proteomic study on Kidney-Yin Deficiency Syndrome patients with diabetes mellitus in China, Acta Pharmacol. Sin. 36 (2015) 689–698, https://doi.org/10.1038/aps.2014.169.
[13] S. Xu, X. Lv, B. Wu, Y. Xie, Z. Wu, X. Tu, H. Chen, F. Wei, Pseudotargeted lipidomics strategy enabling comprehensive profiling and precise lipid structural elucidation of polyunsaturated lipid-rich Echium oil, J. Agric. Food Chem. 69 (2021) 9012–9024, https://doi.org/10.1021/acs.jafc.0c07268.
[14] Q. Xuan, C. Hu, D. Yu, L. Wang, Y. Zhou, X. Zhao, Q. Li, X. Hou, G. Xu, Development of a high coverage pseudotargeted lipidomics method based on ultra-high performance liquid chromatography-mass spectrometry, Anal. Chem. 90 (2018) 7608–7616, https://doi.org/10.1021/acs.analchem.8b01331.
[15] Chinese Diabetes Society, Guideline for the prevention and treatment of type 2 diabetes mellitus in China (2020 edition), Chinese Journal of Practical Internal Medicine 41 (2021) 668–695, https://doi.org/10.19538/j.nk2021080106.
[16] N. Amdanee, M. Shao, X. Hu, X. Fang, C. Zhou, J. Chen, M. Ridwan Chattun, L. Wen, X. Pan, X. Zhang, Y. Xu, Serum metabolic profile in schizophrenia patients with antipsychotic-induced constipation and its relationship with gut microbiome, Schizophr. Bull. 49 (2023) 646–658, https://doi.org/10.1093/schbul/sbac202.
[17] M. Hao, D. Ji, L. Li, L. Su, W. Gu, L. Gu, Q. Wang, T. Lu, C. Mao, Mechanism of curcuma wenyujin rhizoma on acute blood stasis in rats based on a UPLC-Q/TOF-MS metabolomics and network approach, Molecules 24 (2018) 82, https://doi.org/10.3390/molecules24010082.
[18] B. Brügger, Lipidomics: analysis of the lipid composition of cells and subcellular organelles by electrospray ionization mass spectrometry, Annu. Rev. Biochem. 83 (2014) 79–98, https://doi.org/10.1146/annurev-biochem-060713-035324.
[19] S. Zhong, L. Li, X. Shen, Q. Li, W. Xu, X. Wang, Y. Tao, H. Yin, An update on lipid oxidation and inflammation in cardiovascular diseases, Free Radic. Biol. Med. 144 (2019) 266–278, https://doi.org/10.1016/j.freeradbiomed.2019.03.036.

[20] K. Yoshioka, Y. Hirakawa, M. Kurano, Y. Ube, Y. Ono, K. Kojima, T. Iwama, K. Kano, S. Hasegawa, T. Inoue, T. Shimada, J. Aoki, Y. Yatomi, M. Nangaku, R. Inagi, Lysophosphatidylcholine mediates fast decline in kidney function in diabetic kidney disease, Kidney Int. 101 (2022) 510–526, https://doi.org/10.1016/j.kint.2021.10.039.
[21] Z.H. Alshehry, P.A. Mundra, C.K. Barlow, N.A. Mellett, G. Wong, M.J. McConville, J. Simes, A.M. Tonkin, D.R. Sullivan, E.H. Barnes, P.J. Nestel, B.A. Kingwell, M. Marre, B. Neal, N.R. Poulter, A. Rodgers, B. Williams, S. Zoungas, G.S. Hillis, J. Chalmers, M. Woodward, P.J. Meikle, Plasma lipidomic profiles improve on traditional risk factors for the prediction of cardiovascular events in type 2 diabetes mellitus, Circulation 134 (2016) 1637–1650, https://doi.org/10.1161/CIRCULATIONAHA.116.023233.
[22] J.-J. Xu, F. Xu, W. Wang, Y.-F. Zhang, B.-Q. Hao, M.-Y. Shang, G.-X. Liu, Y.-L. Li, S.-B. Yang, X. Wang, S.-Q. Cai, Elucidation of the mechanisms and effective substances of paeoniae radix rubra against toxic heat and blood stasis syndrome with a stage-oriented strategy, Front. Pharmacol. 13 (2022) 842839, https://doi.org/10.3389/fphar.2022.842839.
[23] L. Zong, J. Xing, S. Liu, Z. Liu, F. Song, Cell metabolomics reveals the neurotoxicity mechanism of cadmium in PC12 cells, Ecotoxicol. Environ. Saf. 147 (2018) 26–33, https://doi.org/10.1016/j.ecoenv.2017.08.028.
[24] X. Wang, Y. Xu, X. Song, Q. Jia, X. Zhang, Y. Qian, J. Qiu, Analysis of glycerophospholipid metabolism after exposure to PCB153 in PC12 cells through targeted lipidomics by UHPLC-MS/MS, Ecotoxicol. Environ. Saf. 169 (2019) 120–127, https://doi.org/10.1016/j.ecoenv.2018.11.006.
[25] S.K. Jackson, W. Abate, A.J. Tonks, Lysophospholipid acyltransferases: novel potential regulators of the inflammatory response and target for new drug discovery, Pharmacol. Ther. 119 (2008) 104–114, https://doi.org/10.1016/j.pharmthera.2008.04.001.
[26] S. Cang, R. Liu, W. Jin, Q. Tang, W. Li, K. Mu, P. Jin, K. Bi, Q. Li, Integrated DIA proteomics and lipidomics analysis on non-small cell lung cancer patients with TCM syndromes, Chin. Med. 16 (2021) 126, https://doi.org/10.1186/s13020-021-00535-x.
[27] T. Wang, X. Huang, K. Zhai, J. Yu, J. Li, H. Duan, J. Liu, Z. Lu, J. Guo, F. Li, Integrating metabolomics and network pharmacology to investigate Panax japonicus prevents kidney injury in HFD/STZ-induced diabetic mice, J. Ethnopharmacol. 303 (2023) 115893, https://doi.org/10.1016/j.jep.2022.115893.
[28] J.N. van der Veen, J.P. Kennelly, S. Wan, J.E. Vance, D.E. Vance, R.L. Jacobs, The critical role of phosphatidylcholine and phosphatidylethanolamine metabolism in health and disease, Biochim. Biophys. Acta Biomembr. 1859 (2017) 1558–1572, https://doi.org/10.1016/j.bbamem.2017.04.006.
[29] H. Xue, X. Chen, C. Yu, Y. Deng, Y. Zhang, S. Chen, X. Chen, K. Chen, Y. Yang, W. Ling, Gut microbially produced indole-3-propionic acid inhibits atherosclerosis by promoting reverse cholesterol transport and its deficiency is causally related to atherosclerotic cardiovascular disease, Circ. Res. 131 (2022) 404–420, https://doi.org/10.1161/CIRCRESAHA.122.321253.
[30] S. Rauschert, F.F. Kirchberg, L. Marchioro, B. Koletzko, C. Hellmuth, O. Uhl, Early programming of obesity throughout the life course: a metabolomics perspective, Ann. Nutr. Metab. 70 (2017) 201–209, https://doi.org/10.1159/000459635.
[31] M. El Alwani, B.X. Wu, L.M. Obeid, Y.A. Hannun, Bioactive sphingolipids in the modulation of the inflammatory response, Pharmacol. Ther. 112 (2006) 171–183, https://doi.org/10.1016/j.pharmthera.2006.04.004.
[32] R. Martínez-Beamonte, J.M. Lou-Bonafonte, M.V. Martínez-Gracia, J. Osada, Sphingomyelin in high-density lipoproteins: structural role and biological function, Int. J. Mol. Sci. 14 (2013) 7716–7741, https://doi.org/10.3390/ijms14047716.
[33] Y.-Y. Zhao, H. Miao, X.-L. Cheng, F. Wei, Lipidomics: novel insight into the biochemical mechanism of lipid metabolism and dysregulation-associated disease, Chem. Biol. Interact. 240 (2015) 220–238, https://doi.org/10.1016/j.cbi.2015.09.005.
[34] V. Catalán, G. Frühbeck, J. Gómez-Ambrosi, Inflammatory and oxidative stress markers in skeletal muscle of obese subjects, in: Obesity, Elsevier, 2018, pp. 163–189, https://doi.org/10.1016/B978-0-12-812504-5.00008-8.
[35] E. Barbu, M.-R. Popescu, A.-C. Popescu, S.-M. Balanescu, Inflammation as A Precursor of atherothrombosis, diabetes and early vascular aging, Int. J. Mol. Sci. 23 (2022) 963, https://doi.org/10.3390/ijms23020963.
[36] M.M. Siddique, Y. Li, L. Wang, J. Ching, M. Mal, O. Ilkayeva, Y.J. Wu, B.H. Bay, S.A. Summers, Ablation of dihydroceramide desaturase 1, a therapeutic target for the treatment of metabolic diseases, simultaneously stimulates anabolic and catabolic signaling, Mol. Cell Biol. 33 (2013) 2353–2369, https://doi.org/10.1128/MCB.00226-13.
[37] A.S. Havulinna, M. Sysi-Aho, M. Hilvo, D. Kauhanen, R. Hurme, K. Ekroos, V. Salomaa, R. Laaksonen, Circulating ceramides predict cardiovascular outcomes in the population-based FINRISK 2002 cohort, Arterioscler. Thromb. Vasc. Biol. 36 (2016) 2424–2430, https://doi.org/10.1161/ATVBAHA.116.307497.
[38] H. M, Role of impaired glycolysis in perturbations of amino acid metabolism in diabetes mellitus, Int. J. Mol. Sci. 24 (2023), https://doi.org/10.3390/ijms24021724.
[39] X. Mao, R. Sun, Q. Wang, D. Chen, B. Yu, J. He, J. Yu, J. Luo, Y. Luo, H. Yan, J. Wang, H. Wang, Q. Wang, l-Isoleucine administration alleviates DSS-induced colitis by regulating TLR4/MyD88/NF-κB pathway in rats, Front. Immunol. 12 (2021) 817583, https://doi.org/10.3389/fimmu.2021.817583.
[40] C.E. Mountford, L.C. Wright, Organization of lipids in the plasma membranes of malignant and stimulated cells: a new model, Trends Biochem. Sci. 13 (1988) 172–177, https://doi.org/10.1016/0968-0004(88)90145-4.
[41] K. Sonkar, V. Ayyappan, C.M. Tressler, O. Adelaja, R. Cai, M. Cheng, K. Glunde, Focus on the glycerophosphocholine pathway in choline phospholipid metabolism of cancer, NMR Biomed. 32 (2019) e4112, https://doi.org/10.1002/nbm.4112.
[42] D. Hanahan, R.A. Weinberg, Hallmarks of cancer: the next generation, Cell 144 (2011) 646–674, https://doi.org/10.1016/j.cell.2011.02.013.
[43] L. Schiffer, L. Barnard, E.S. Baranowski, L.C. Gilligan, A.E. Taylor, W. Arlt, C.H.L. Shackleton, K.-H. Storbeck, Human steroid biosynthesis, metabolism and excretion are differentially reflected by serum and urine steroid metabolomes: a comprehensive review, J. Steroid Biochem. Mol. Biol. 194 (2019) 105439, https://doi.org/10.1016/j.jsbmb.2019.105439.